

1 **Building new compartments for unconventional protein secretion from the early and late**
2 **Golgi membranes**

3

4 Amy J. Curwin¹, Nathalie Brouwers¹, Akihiko Nakano⁴, Kazuo Kurokawa⁴ and Vivek
5 Malhotra^{1,2,3*},

6

7

8

9 ¹Centre for Genomic Regulation, The Barcelona Institute of Science and Technology, 08003
10 Barcelona, Spain

11 ²Universitat Pompeu Fabra (UPF), 08002 Barcelona, Spain

12 ³ICREA, 08010 Barcelona, Spain

13 ⁴Live Cell Super-Resolution Imaging Research Team, RIKEN Center for Advanced Photonics,
14 Wako, Saitama, Japan.

15

16

17

18 **CUPS, a compartment for unconventional secretion of signal sequence lacking proteins, is**
19 **built during starvation. CUPS, lacking the Golgi specific glycosyltransferases, form by**
20 **COPI independent extraction of membranes from the early Golgi cisterna, require PI4P**
21 **for their biogenesis and PI3P for stability. We now show that a PI4P effector Drs2 of the**
22 **trans-Golgi network, relocates to a new compartment monikered TCUPS because it**
23 **touches CUPS. Although localized to TCUPS, Drs2 is required for CUPS formation**
24 **specifically by interacting with Rcy1, and this process is essential for unconventional**
25 **secretion. Visualizing cells by 4D SCLIM technology revealed that tubules emanating from**
26 **TCUPS are often collared by CUPS and severed. Incidentally, while CUPS are stable,**
27 **TCUPS are vesiculated at late stages of starvation. This mirrors the dynamics of the early**
28 **and late Golgi during conventional protein secretion. TCUPS and CUPS thus emerge as the**
29 **functional equivalent of early and late Golgi of the conventional secretory pathway, thus**
30 **representing key compartments in unconventional secretion.**

31

32

33 **Introduction**

34 The problem of how proteins that cannot enter the endoplasmic reticulum (ER)-Golgi pathway of
35 secretion are released to the extracellular space remains a fascinating challenge. This is an
36 important issue because cells secrete proteins like fibroblast growth factor (FGF) 2, Interleukin
37 (IL)-1 β , Acyl CoA binding protein (Acb1/Diazepam binding inhibitor), Superoxide dismutase
38 (SOD) 1, and tissue transglutaminase, which have important physiological roles in the
39 extracellular space, particularly under conditions of stress. The prevailing schemes for the
40 secretion of this class of cytoplasmic proteins include: involvement of an intracellular
41 compartment, such as CUPS (compartment for unconventional protein secretion), for proteins
42 like Acb1, SOD1 and many other antioxidants, or secretory endosomes or lysosomes, in the case
43 of fatty acid binding protein 4 (FABP4), or direct translocation across the plasma membrane for
44 FGF2 (Bruns et al., 2011; Cruz-Garcia et al., 2020; Schäfer et al., 2004; Villeneuve et al., 2017).
45 IL-1 β is reported to use multiple routes of export such as translocation directly across the plasma
46 membrane via a pore created by Gasdermin D, translocation by conventional cargo receptor
47 protein TMED10 into the ER-Golgi intermediate compartment (ERGIC) prior to its release from
48 cells, and by pyroptosis (He et al., 2015; Liu et al., 2016; Zhang et al., 2020).

49 There might indeed be different routes for this mode of transport, but we have focussed
50 on the pathway for secretion of Acb1 and Sod1. The export of these proteins has the following
51 essential requirements. 1, Their secretion is triggered upon carbon and nitrogen starvation, and
52 growth in potassium acetate; 2, intracellular production of reactive oxygen species (ROS); 3, the
53 need of a peripherally Golgi/ER exit site localized protein called Grh1 (GORASPs in mammals);
54 and 4, a compartment called CUPS (Bruns et al., 2011; Cruz-Garcia et al., 2014, 2020; Curwin et
55 al., 2016; Kinseth et al., 2007). It is of note that release of IL-1 β is also dependent on GORASP

56 proteins in LPS activated macrophages (Chiritoiu et al., 2019). GORASP is a key to unravelling
57 this process because so far it is the only proteins that is required for many types of
58 unconventional secretion of several different proteins in organisms through evolution, from yeast
59 to mammals (add refs here).

60 In yeast, CUPS is marked by the presence of the single GORASP orthologue, Grh1
61 (Bruns et al., 2011). CUPS forms independent of COPI and COPII proteins, but requires the
62 function of the phosphatidylinositol (PI) 4-kinase, Pik1, of the late Golgi membranes or trans-
63 Golgi network (TGN) (Cruz-Garcia et al., 2014). During the time course of starvation, and
64 correlating with the timing of unconventional secretion, CUPS “mature”, ultimately acquire large
65 enveloping membranes in a process that requires the function of the PI 3-kinase, Vps34 and a
66 subset of ESCRT proteins. In the absence of Vps34 or ESCRT complexes I, II, or III CUPS
67 initially form, but later fragment. The major subunit of ESCRT-III, Snf7, also transiently
68 localizes to the CUPS (Curwin et al., 2016).

69 We now report that that Drs2, a PI4P effector that functions as an aminophospholipid
70 flippase and localized at the TGN in growth, is essential for CUPS biogenesis. This requirement
71 in CUPS biogenesis is dependent on its binding partner Rcy1. Our data reveal that during
72 unconventional secretion, cells create a new, TGN-derived compartment that is enriched in Drs2,
73 Tlg2 (t-SNARE) and Snc2 (v-SNARE), which transiently contacts Grh1 containing CUPS. We
74 have called this new compartment TCUPS for Touching CUPS. 4D imaging of cells by SCLIM
75 revealed that CUPS and TCUPS make numerous, but transient contacts. Tubules emanating from
76 TCUPS are often collared by CUPS. In some cases, the tubule appears to be severed post-
77 contact. We believe these contacts are essential during the stress of starvation to facilitate

78 compartment formation, maturation and stability of both CUPS and TCUPS. The discussion of
79 our findings follows.

80

81

82 **Results**

83

84 **PI4P effector Drs2 is necessary for CUPS biogenesis**

85 PI4P is produced at the TGN by the PI 4-kinase Pik1 and is essential for proper Golgi function
86 via various PI4P dependent pathways (Graham and Burd, 2011; Walch-Solimena and Novick,
87 1999). By use of a temperature sensitive allele, Pik1 was previously shown to be required for
88 efficient CUPS biogenesis, however a PI4P fluorescent sensor does not localize to the Golgi, but
89 is diffusely dispersed in the cytoplasm under these starvation conditions, indicating a decrease of
90 Golgi PI4P levels (Cruz-Garcia et al., 2014). This is in accordance with published work
91 indicating that glucose starvation leads to a rapid decrease of Golgi PI4P via re-localization of
92 the enzymes, Pik1 and the Sac1 PI 4-phosphatase (Demmel et al., 2008; Faulhammer et al.,
93 2007). This therefore begs the question: what is the function of the late Golgi and Pik1 in the
94 overall process of CUPS formation and what are the effectors of PI4P in this pathway?

95 The multi-spanning transmembrane protein Drs2, aminophospholipid flippase, is a PI4P
96 effector localized at the TGN membranes. We examined location of genomically expressed
97 Grh1-2xmCherry and Drs2-3xGFP in growth and throughout the time course of starvation by
98 confocal live spinning disk microscopy. In growth, Drs2 labelled 4-6 punctae per cell that were
99 often apposed to but not colocalized with Grh1 (Figure 1A). Upon starvation, Grh1 re-localized
100 to 1-3 larger foci, which we have shown previously to be the CUPS. Curiously, Drs2 also re-
101 localized to 1-3 larger foci per cell and in addition displayed faint diffuse localization throughout

102 the cytoplasm (Figure 1A). The foci of Grh1 and Drs2 were never observed to be stably
103 localized, however, transient co-localization of the foci was frequently observed, particularly
104 early in starvation (26% of cells). The rate of transient co-localization decreased throughout the
105 time course of starvation (10% of cells), however this could be a reflection of the fact that the
106 overall number of Drs2 compartments also decreased throughout starvation. The average number
107 of Drs2 structures per cell decreased from 2.3/cell in the first 45 min to 1.5/cell in the last 30 min
108 of starvation, while the average percentage of cells with no Drs2 structures increased from 7.9%
109 to 13.8% in the same time period (Figure 1).

110 Next, we asked if Drs2 contributed to the process of CUPS formation. We examined
111 localization of Grh1-2xGFP in cells lacking Drs2 and found a strong defect in CUPS biogenesis
112 as observed by Grh1 localized to numerous smaller structures (Figure 1B). After 2.5-3 hours of
113 starvation, CUPS were still unable to form in the absence of Drs2.

114

115 **Drs2 functions specifically with Rcy1 in CUPS formation**

116 Drs2, a multi-spanning transmembrane protein functions at the TGN to flip mainly
117 phosphatidylserine (PS), but also phosphatidylethanolamine (PE) to maintain phospholipid
118 asymmetry and drive vesicle formation (Chen et al., 1999; Gall et al., 2002; Hua et al., 2002; Liu
119 et al., 2008; Natarajan et al., 2004). The C-terminal domain of Drs2 has an autoinhibitory
120 function that is relieved specifically upon binding of PI4P. Interaction of Drs2 with Arf-GEF
121 Gea2 and Arf-like GTPase Arl1 are also critical in regulating multiple clathrin-dependent,
122 anterograde pathways (Bai et al., 2019; Hankins et al., 2015; Natarajan et al., 2009; Timcenko et
123 al., 2019; Tsai et al., 2013; Zhou et al., 2013). Clathrin and the PI4P sensor dissociate from the
124 TGN upon starvation, we therefore did not expect a role for these players in CUPS formation.

125 Regardless, Gea2, Arl1 and clathrin (clathrin heavy chain or adaptor proteins) mutant strains
126 lacking the function of these proteins were tested and revealed no effect on CUPS formation
127 (Figure S1). Drs2, via its interaction to Rcy1, also regulates a retrograde pathway required for
128 recycling of exocytic v-SNAREs Snc1 to the TGN. This interaction is also via the C-terminal
129 domain of Drs2 in a region proximal to the PI4P binding site, and partially overlapping with the
130 Gea2 binding site (Furuta et al., 2006; Hanamatsu et al., 2014). Deletion of *RCY1* resulted in
131 highly vesiculated Grh1-positive structures, exactly as for loss of Drs2, clearly indicating the
132 Drs2-Rcy1 branch of Drs2 function is specifically required for CUPS formation (Figure 2A).

133

134 **CUPS formation requires v-SNARE function**

135 A major known function of the Drs2-Rcy1 pathway is recycling of the exocytic v-SNARE Snc1,
136 we asked if Snc1 is also required for CUPS formation. Snc1 and Snc2 are the only post-Golgi v-
137 SNAREs in yeast and form an essential pair with redundant functions in cell growth and
138 secretion (Protopopov et al., 1993). Single gene deletion of either produced no phenotype in
139 CUPS formation (Figure S1). However, a double mutant temperature-sensitive strain lacking
140 Snc1 and with Snc2 mutated to be inefficiently recycled from the plasma membrane, *snc2*-
141 *V39A,M42A*, (Shen et al., 2013) displayed the highly vesiculated CUPS phenotype, even without
142 temperature shift (Figure 2). The double mutant cells grew in normal conditions, but the sole
143 mutated v-SNARE, Snc2, did not support formation of CUPS upon starvation.

144 Is the defect in CUPS due to a defect in recycling of v-SNAREs to the TGN or more
145 directly related to the function of Drs2/Rcy1? Yeast have a minimal endomembrane system and
146 an early TGN, marked specifically by the presence of the t-SNARE Tlg2, likely serves as an
147 early endosome, while a later TGN is the site of exocytosis and clathrin-coated vesicle formation

148 (Day et al., 2018; Tojima et al., 2019). The recycling of Snc1 to the early TGN has been shown
149 to follow 3 distinct pathways; Drs2-Rcy1, that sort the Snc1 from the early endosome-like TGN,
150 while the sorting nexins Snx4 and Atg20, as well as retromer, sort v-SNAREs at late endosomes
151 (or the prevacuolar compartment in yeast), although retromer likely only becomes important
152 when the other 2 pathways are not functioning (Best et al., 2020; Hanamatsu et al., 2014; Ma and
153 Burd, 2019). We tested these pathways in CUPS biogenesis and observed no defect in cells
154 lacking the sorting nexins Snx4 and Atg20, or the retromer subunit, Vps35 (Figure 2). Therefore,
155 the defect observed in Drs2/Rcy1 deleted cells is not simply due to loss of v-SNARE pool at the
156 TGN. The combined data suggest that CUPS specifically require membranes from an early
157 endosome-like TGN compartment, in Drs2/Rcy1 dependent manner.

158

159 **Rcy1 and Snc1/Snc2 are required for unconventional secretion**

160 Unconventional secretion in yeast leads to some secreted proteins being trapped in the cell wall
161 or periplasmic space and to measure this secretion a mild cell wall extraction procedure is
162 necessary to prevent cell lysis associated with perturbations to the rigidity of the cell wall
163 (Curwin et al., 2016). As such, any genetic mutations or treatments (such as temperature shift)
164 that exacerbate this problem of lysis cannot be tested by this assay to score unconventional
165 secretion. Cells lacking Drs2 have numerous defects, particularly in lipid homeostasis (Hankins
166 et al., 2015) and therefore could not be tested (data not shown). However, *rcy1* Δ cells do not
167 exhibit as many defects associated with loss of Drs2 function, therefore we tested their capacity
168 to secrete unconventional cargoes such as Acb1, and the antioxidants Sod1 and Trx2. Wild type
169 and *rcy1* Δ cells were starved for 2.5 hours after which the secreted material was extracted from
170 the cell wall, as described previously (Curwin et al., 2016). The intracellular and secreted

171 fractions were probed by western blot for the various cargoes, Cof1-which is used to monitor cell
172 lysis, and the known cell wall protein Bgl2. Loss of Rcy1 led to a strong defect in release of
173 Acb1, Sod1 and Trx2 without causing release of cytoplasmic content measured by the lack of
174 Cof1 presence (Figure 3A). Similarly, the v-SNARE double mutant defective in CUPS formation
175 (Figure 2) was tested and also exhibited a reduction in secretion of Acb1, Sod1 and Trx2 (50-
176 60% compared to control cells) (Figure 3B). Therefore, we can conclude that unconventional
177 secretion in starvation requires Rcy1 (presumably in concert with Drs2) and v-SNARE activity,
178 but the precise function of these players remains to be determined.

179

180 **Drs2 and the SNARE proteins Snc2 and Tlg2 label a new compartment that transiently**
181 **contacts CUPS**

182 We generated N-terminal GFP fusions of the v-SNAREs, Snc1 and Snc2, and their cognate t-
183 SNARE, Tlg2, which preferentially labels the early TGN and therefore likely receives the v-
184 SNARE vesicles being recycled in a Drs2-Rcy1 dependent manner. Most analyses of v-SNARE
185 itinerary have been performed by overexpression of an N-terminal GFP tagged Snc1, that at
186 steady-state labels mostly the plasma membrane of growing buds and some internal structures
187 (Lewis et al., 2000). Recently, Graham and colleagues generated an mNG-Snc1 construct
188 expressed at much lower levels, which preferentially labelled the TGN and endosomes (Best et
189 al., 2020). To avoid plasmid overexpression altogether, we integrated the GFP tag at the N-
190 terminus of each SNARE, at its endogenous locus, under the control of Sed5 promoter.

191 Interestingly, a different steady state pattern for Snc1 and Snc2 was observed during growth. The
192 overall signal of Snc1 was weaker than that of Snc2, and distinct localization of Snc1 was only
193 observed in the tips of very small budded cells and somewhat in the necks of large budded cells

194 (Figure 4A). Unbudded and large/medium budded cells displayed mostly a diffuse signal of
195 Snc1. Snc2, on the other hand, exhibited distinct localization in all cells, preferentially labelling
196 mostly internal structures, the neck of large budded cells, and occasionally the plasma membrane
197 of small and medium budded cells (Figure 4A). So, although the v-SNAREs are redundant in
198 function they clearly have their own preferred steady-state itineraries. Tlg2 localized as expected
199 in growth, labelling 4-6 punctae per cell (Figure 4A). None of the SNARE proteins could be co-
200 localized with Grh1 in growth conditions.

201 Upon starvation the Snc1 signal rapidly became diffuse in most cells (less than 5%
202 retained 1-2 faint foci) indicating Snc1 is the preferred v-SNARE for exocytosis. In contrast, the
203 Snc2 signal remained high in all cells, labelling fewer and larger punctate elements (Figure 4B).
204 Tlg2 also labelled fewer and larger structures immediately upon starvation, in the same manner
205 as Drs2. Both Snc2 and Tlg2 structures could be found transiently co-localized with Grh1
206 (Figure 4B). In the case of Snc2, this was observed on average in 13% of cells at any particular
207 time point in starvation, while Tlg2 co-localization with Grh1 was more frequent early in
208 starvation (14% of cells early and 7% of cells later in starvation), similar to Drs2. Examination of
209 GFP-Tlg2 with Drs2-3xCherry revealed that they are indeed contained in the same compartment
210 in starvation (Figure S2). Drs2 could be predicted to be in both the early and late TGN
211 membranes due its function in anterograde and retrograde transport, while Tlg2 is specific to
212 early TGN. We observed a partial co-localization in growth conditions, as expected if this were
213 true (Figure S2). In starvation, the number of TGN membranes was reduced and the co-
214 localization of Drs2 and Tlg2 was greatly increased (Figure S2). The same was also observed
215 when mCherry-Snc2 and GFP-Tlg2 were tested for their location during starvation. The signal of
216 mCherry-Snc2 was very weak compared to the GFP version, but larger Snc2 structures were

217 observed to co-localize with Tlg2 (Figure S2). Therefore, starvation induces the formation of a
218 new compartment derived from the early TGN that is enriched Drs2, Tlg2 and Snc2. We now
219 discuss data showing this new compartment contacts CUPS transiently and based on this feature
220 we have called it TCUPS for Touching CUPS.

221

222 **SCLIM reveals the process of CUPS formation in 4D**

223 We previously presented the ultra-structure of CUPS using CLEM (correlative light electron
224 microscopy) as a spherical tubulovesicular structure that grows in overall size during starvation
225 and acquires a large enveloping cup-shaped cisternae (Curwin et al., 2016). To gain better insight
226 into the organization of membranes that compose CUPS and its potential interaction with
227 TCUPS we used super-resolution confocal live imaging (SCLIM) (Kurokawa et al., 2013, 2019).
228 SCLIM analysis of Grh1-2xGFP has confirmed these structures and further revealed their
229 dynamic behaviour (Figure 5 and Movies1-4). Grh1 was localized to many small and mobile
230 structures in growth conditions. Detailed analysis of larger Grh1-positive structures at 3 hours
231 starvation revealed mature CUPS could be categorized in 3 forms; spherical, cup-like and curved
232 (Figure 5B). Even though the overall mobility of structures decreased during the time course of
233 starvation, the CUPS morphology could dynamically change between the different forms (Movie
234 1). Dynamic Grh1 structures could be observed to contact each other at times, possibly fusing
235 and becoming more stable (Figure 5C and Movies1-4). Moreover, a subsequent analysis earlier
236 in starvation (1 - 1.5 hour), indicated dynamic Grh1-positive structures contacted numerous
237 times, growing in size likely by fusion, as well larger Grh1 structures could also be observed to
238 fragment at times (Movies S1-3). Altogether, the SCLIM analyses reveal that CUPS form by
239 dynamic interactions between Grh1 containing membranes, which likely involves fusion and

240 fission. These highly dynamic interactions then reach a steady state and generate a more stable
241 CUPS.

242

243 **Dynamics of Drs2 compartment (TCUPS) and contacts to CUPS**

244 Before monitoring Grh1 in combination with other proteins by SCLIM, we observed the changes
245 in the TGN compartments induced upon starvation and the formation of TCUPS. We therefore
246 examined of the organization of Drs2-3xmCherry and GFP-Tlg2 in growth and starvation. Tlg2
247 localizes to an early TGN compartment while. In growth, co-localization of Drs2 and Tlg2 was
248 observed in some cisternae, but not all. Following the structures over time revealed an order of
249 events, with structures first labelled by Tlg2, then acquiring Drs2 (co-localization), subsequently
250 losing Tlg2, and finally the loss of Drs2 (Figure 6A and Movie 5). In starvation, the extent of
251 Drs2 and Tlg2 co-localization was greatly increased as TCUPS form. Interestingly, the same
252 dynamics could be observed in starvation, with structures only marked by Tlg2 then acquiring
253 Drs2, followed by Drs2 alone, and finally the loss if TCUPS compartment (Figure 6B and
254 Movies 6-8).

255

256 **Fragmentation of TCUPS by contact with CUPS**

257 Finally, we analyzed the dynamics of Grh1-2xmCherry containing CUPS in combination with
258 Drs2-3xGFP, GFP-Tlg2 or GFP-Snc2 to visualize the CUPS-TCUPS interaction. SCLIM
259 analysis captured numerous contacts between CUPS and TCUPS. These contacts were not
260 observed frequently, but given they are transient they are likely difficult to capture. The nature of
261 contacts often involved insertion of a TCUPS tubule into CUPS. This could be observed with
262 Drs2, Tlg2 or Snc2 as the marker of TCUPS. In Figure 7A and Movie 9 an example with Drs2 is

263 provided, where the Drs2-positive membranes inserted into CUPS and fragments were produced.
264 In another remarkable movie, with Tlg2 as the TCUPS marker, the CUPS collar and appear to
265 sever a tubule derived from TCUPS, although direct cutting of TCUPS by CUPS cannot be
266 conclusively stated by this analysis alone (Figure 7B and Movie 10). In addition to TCUPS,
267 Snc2, and to a lesser extent Drs2, also labelled numerous smaller structures that also often
268 contacted with or were in the vicinity of CUPS (Figure S3 and Movies S4-8). These are likely
269 vesicles/tubules, as Drs2 itself has been shown to be packaged into vesicles during its activity
270 (Liu et al., 2008). The combined evidence suggests that TCUPS is being consumed during
271 starvation in the process of vesicle formation, driven, at least partially, by the action of Drs2-
272 Rcy1. Although these vesicles are not fusing directly to the CUPS, as we do not observe this by
273 SCLIM, the absence of Drs2-Rcy1 activity is essential for both CUPS formation and
274 unconventional secretion.

275

276

277 **Discussion**

278 George Palade mapped the pathway of protein secretion, which laid the foundation for decades
279 of research on how proteins are exported from the ER and transported via the Golgi complex to
280 their ultimate destinations. Blobel revealed how proteins enter this ER-Golgi pathway of
281 secretion via the N-terminal signal sequence. The knowledge that eukaryotic cells secrete
282 proteins lacking the N-terminal signal sequence and therefore cannot follow the Blobel-Palade's
283 pathway of protein secretion is also beginning to receive attention. This unconventional secretory
284 pathway releases a large and diverse class of proteins with varied vital physiological functions in
285 extracellular space for immune surveillance, tissue reorganization, insulin homeostasis, and
286 protection from oxidative damage, for example. We showed that the Golgi associated protein

287 GORASP, is required for the secretion of Acb1 in nutrient-starved *Dictyostelium discoideum*
288 (Kinseth et al., 2007). This function of GORASP (a single gene in invertebrates, two genes in
289 vertebrates) is now known to be conserved. We have focused on the pathway of GORASP-
290 dependent unconventional secretion and our findings have led to identification of a compartment
291 that we call CUPS, which is synthesized under the conditions that trigger unconventional
292 secretion (Bruns et al., 2011; Cruz-Garcia et al., 2014). CUPS are composed of membranes
293 recruited from the Golgi apparatus, identified by the presence of Grh1 (GORASP ortholog in
294 yeast), and form without the function of COPI and COPII components. CUPS formation depends
295 on the phosphoinositides PI4P for biogenesis and PI3P for its stability. The major ESCRT-III
296 protein Snf7 is also found at the CUPS transiently (Curwin et al., 2016). Importantly, all of these
297 molecular components are also required for secretion of Acb1, Sod1 and Trx2 (Cruz-Garcia et
298 al., 2020; Curwin et al., 2016).

299
300 Our new findings reveal that PI4P functions in the requirement of Drs2, a transmembrane
301 aminophospholipid flippase, in both CUPS formation and unconventional secretion. Of the many
302 proteins that function with Drs2 in trafficking at the TGN that includes Gea2, Arl1 and Rcy1,
303 only Rcy1 is involved in unconventional secretion. We also report a requirement for v-SNARE
304 function (Snc1 and Snc2 orthologous pair) in CUPS formation and unconventional secretion.
305 Together, the starving yeast generate a single new compartment from the TGN that contains
306 Drs2, the v-SNARE Snc2 (but not Snc1) and the t-SNARE Tlg2. This compartment that we have
307 called TCUPS contacts Grh1 containing CUPS.

308

309 **Building and remodeling TCUPS during unconventional protein secretion.**

310 Live cell 4D imaging (SCLIM) has revealed membrane contacts between CUPS and TCUPS.
311 The contacts are transient and highly dynamic, with CUPS membranes often observed to enwrap
312 or encircle TCUPS. We have captured a fascinating event in the contact of CUPS to TCUPS: a
313 tubule emerging from TCUPS is collared by CUPS and appears to be severed. This event is
314 reminiscent of the contact of ER and the endosomes and the fission of the latter compartment
315 (Rowland et al., 2014). We have previously shown that Snf7, a protein of the ESCRT III
316 complex, is recruited transiently to CUPS. However, Vps4 is not required for CUPS biogenesis
317 or for the secretion of Acb1. We propose that CUPS collar the neck of a TCUPS derived tubule
318 and Snf7 located at this junction is involved in events leading to the severing of the respective
319 tubule. There is at least one example of ESCRT mediated severing of a tubule on the cytoplasmic
320 face of a membrane bound compartment (McCullough et al., 2015).

321

322 **Unconventional secretion aping conventional secretion.**

323 In Palade's conventional secretory pathway, proteins destined for secretion are translocated into
324 the ER lumen, folded and sorted, transported to the Golgi, and from there on to their final
325 destinations. Unconventionally secreted cargoes are not glycosylated so they do not need to enter
326 the ER. But there is still the question of how a fraction of this class of proteins is selected and
327 translocated from the cytoplasm for their subsequent delivery to the extracellular space. Our data
328 reveal that membranes from the Golgi and the TGN are extracted by COPI-, COPII-, and
329 clathrin-independent pathway to create two distinct compartments (Figure 8). These are marked
330 by: 1, Grh1 (previously defined as CUPS) and 2, Drs2/Tlg2/Snc2 (TCUPS). CUPS and TCUPS
331 are therefore the early and late Golgi equivalent of the unconventional secretory pathway. The
332 only obvious difference being that they do not contain the Golgi specific glycosylating enzymes.

333 We have shown previously that CUPS contain Acb1, but this has only been observed with
334 immunoelectron microscopy. We admit that we do not know if Acb1 enters directly into CUPS.
335 CUPS and TCUPS transiently contact and it is possible that Acb1 is transferred from CUPS to
336 TCUPS during their transient connection. TCUPS, we suggest are the sorting station for the
337 cargo. How this is achieved is also not known. We have seen that CUPS collar a tubule
338 emanating from TCUPS. Snf7 of the ESCRT pathway that is also recruited transiently to CUPS
339 might be involved in generating and or severing this tubule from TCUPS. Are the tubules
340 enriched in cargo destined to the cell surface? Over time, TCUPS are completely fragmented
341 Much like the TGN during the conventional protein secretion. In the end this arrangement of
342 creating new compartments is used by cells to deliver essential activities to the extracellular
343 space during starvation. Upon return to the normal growth conditions, the remaining CUPS are
344 reabsorbed to the ER by a COPI dependent manner. This is reminiscent of COPI dependent
345 retrograde transport to the ER under growth conditions.

346 In sum, during starvation, the cells use the preexisting Golgi membrane to create new
347 compartments for capturing cytoplasmic proteins, their sorting and the export for secretion. This
348 foundational scheme provides a means to address the mechanism of unconventional protein
349 secretion.

350

351 **Materials and Methods**

352

353 **Yeast strains and media**

354 Yeast cells were grown in synthetic complete (SC) media (0.67% yeast nitrogen base without

355 amino acids, 2% glucose supplemented with amino acid drop-out mix from ForMedium). All

356 strains are derived from the BY4741 background (*MATa his3Δ1 leu2Δ0 met15Δ0 ura3Δ0*).

357 Deletion strains were from the EUROSCARF collection with individual genes replaced by

358 KanMx4. Strains expressing C-terminally 2xyeGFP- and/or 2xyomCherry-tagged Grh1 were

359 constructed by a PCR-based targeted homologous recombination and have been described

360 previously (Cruz-Garcia et al., 2014). In many cases, strains were generated by mating and

361 sporulation, followed by selection of clones with appropriate markers, and confirmation of

362 haploidy. The double mutant v-SNARE (BY4741 *snc1Δ::kanMX4 snc2-V39A,M42A*) strain was

363 provided by Peter Novick. This mutant expressing Grh1-2xyeGFP was generated by mating,

364 sporulation and confirmation of markers and temperature sensitivity. Drs2-3xGFP, KanMx4

365 strain was a gift from Oriol Gallego (UPF).

366

367 *Construction of N-terminally tagged SNAREs*

368 The plasmid pYM-N9 (PCR toolbox) was used to generate a new template vector for PCR-based

369 integration containing the NatNT2 selection cassette, the promoter of Sed5, followed by 2

370 tandem yeGFP. The promoter of Sed5 was amplified from genomic DNA with primers “SacI

371 PrSed5 Fw1”: ATAGAGCTCTTACCATGTCCTCCAGAATTACGA and “XbaI PrSed5 Rv1”:

372 TCATCTAGAGGGAGTTGTGTGGTATGGTG to generate a 658 bp fragment and was cloned

373 into pYM-N9, replacing the high expression *ADHI* promoter. Subsequently a second yeGFP

374 fragment was generated using primers “XbaI ATG yeGFP”:
375 TGATCTAGAAAAAATGTCTAAAGGTGAAGAATTATTCCTGG and “EcoRV non-stop
376 yeGFP”: TCTGATATCAGGCCTCATCGATGAATTCTCTGTCGGA and cloned downstream
377 of the first yeGFP. Finally, standard S1/S4 primers were used to generate the N-terminal
378 integration fragment targeting the Snc1, Snc2 and Tlg2 loci. Strains were confirmed as positive
379 by microscopy and PCR to confirm the presence of 2 yeGFP. In most cases, however only one
380 GFP integrated and the resulting 1xyeGFP strains were used. In the case of Snc1, 2xyeGFP was
381 initially analyzed and subsequently a single yeGFP version was generated and found to behave in
382 an identical manner as the 2xyeGFP version. SnapGene software (from GSL Biotech, Chicago,
383 IL; available at www.snapgene.com) was used for molecular cloning design.

384

385 **Antibodies**

386 All antibodies were raised in rabbit and have been described previously. Anti-Sod1 and anti-Trx2
387 were the kind of gifts of Yoshiharu Inoue (Research Institute for Food Science, Kyoto
388 University) and T. O’Halloran (Northwestern University, Chicago, IL), respectively. Anti-Cof1
389 was kindly provided by John Cooper (Washington University in St. Louis) and anti-Bgl2 was a
390 gift from Randy Schekman (UC Berkeley). Anti-Acb1 antibody was generated by inoculating
391 rabbits with recombinant, untagged Acb1, purified from bacteria and has been described
392 previously (Curwin et.al 2016). HRP conjugated anti-rabbit secondary was from Jackson
393 Immunoresearch (Cat# 711-035-152).

394

395

396

397 **Cell wall extraction assay**

398 Yeast cells were inoculated at a density of 0.003-0.006 OD₆₀₀/mL in SC medium at 25°C. The
399 following day, when cells had reached OD₆₀₀ of 0.4-0.7 equal numbers of cells (16 OD₆₀₀ units)
400 were harvested, washed twice in sterile water, resuspended in 1.6 mL of 2% potassium acetate
401 and incubated for 2.5 hours. When growing cells were to be analyzed 16 OD₆₀₀ units were
402 directly harvested. The cell wall extraction buffer (100mM Tris-HCl, pH 9.4, 2% sorbitol) was
403 always prepared fresh before use and kept on ice. To ensure no loss of cells and to avoid cell
404 contamination in the extracted buffer, 2mL tubes were siliconized (Sigmacote) prior to
405 collection. Cells were harvested by centrifugation at 3000xg for 3 minutes at 4°C, medium or
406 potassium acetate was removed and 1.6 mL of cold extraction buffer was added. Cells were
407 resuspended gently by inversion and incubated on ice for 10 minutes, after which they were
408 centrifuged as before, 3000xg for 3 minutes at 4°C, and 1.3 mL of extraction buffer was removed
409 to ensure no cell contamination. The remaining buffer was removed and the cells were
410 resuspended in 0.8 mL of cold TE buffer (Tris-HCl, pH 7.5, EDTA) with protease inhibitors
411 (aprotinin, pepstatin, leupeptin (Sigma)) and 10 µL was boiled directly in 90 µL of 2x sample
412 buffer (lysate). For western blotting analysis, 30 µg of BSA (bovine serum albumin (Sigma))
413 carrier protein and 0.2 mL of 100% Trichloroacetic acid (Sigma) was added to the extracted
414 protein fraction. Proteins were precipitated on ice for 1 hour, centrifuged 16,000xg for 30
415 minutes and boiled in 50 µL 2x sample buffer. For detection, proteins (10 µL each of lysate or
416 wall fractions) were separated in a 12% polyacrylamide gel before transfer to 0.2 µm
417 nitrocellulose (GE Healthcare) for detection by western blotting. For preparation of cell wall
418 extracts for mass spectrometry analysis, no BSA carrier protein was added and the proteins were
419 precipitated with acetone and not TCA.

420 **Epifluorescence microscopy**

421 After incubation in the appropriate medium cells were harvested by centrifugation at 3,000 g for
422 3 min, resuspended in a small volume of the corresponding medium, spotted on a microscopy
423 slide, and imaged live with a DMI6000 B microscope (Leica) equipped with a DFC 360FX
424 camera (Leica) using an HCX Plan Apochromat 100x 1.4 NA objective. Images were acquired
425 using LAS AF software (Leica) and processing was performed with ImageJ 1.47n software.

426

427 **Spinning disk confocal fluorescence microscopy**

428 After incubation in starvation medium for 20 min, ~0.05 OD_{600nm} of cells were plated in
429 starvation medium on Concanavalin A-coated (Sigma-Aldrich) Lab-Tek chambers (Thermo
430 Fisher Scientific) and were allowed to settle for 20 min at 25°C. Cells were continuously imaged
431 up to 10 min throughout starvation. Whole cell Z stacks with a step size of 0.4 μm were
432 continuously acquired (10 sec frames) using a spinning-disk confocal microscope (Revolution
433 XD; Andor Technology) with a Plan Apochromat 100× 1.45 NA objective lens equipped with a
434 dual-mode electron-modifying charge-coupled device camera (iXon 897 E; Andor Technology)
435 and controlled by the iQ Live Cell Imaging software (Andor Technology). Some later images
436 were taken on a newer spinning disk system (Andor Dragonfly) equipped with a 488nm and/or
437 561nm diode, using a U Plan Apo 60x 1.4 oil objective and an iXON-EMCCD Du-897 camera.
438 A 2x camera zoom was used to reach Nyquist sampling, Fusion software was used for
439 acquisition. Post-acquisition processing was performed with ImageJ 1.47n software.

440

441

442

443 **SCLIM (super resolution confocal live imaging)**

444 For high-speed live imaging, yeast cells were immobilized on glass slides using concanavalin A
445 and imaged by SCLIM. SCLIM was developed by combining Olympus model IX-71 inverted
446 fluorescence microscope with a UPlanSApo 100× NA 1.4 oil objective lens (Olympus), a high-
447 speed and high signal-to-noise ratio spinning-disk confocal scanner (Yokogawa Electric), a
448 custom-made spectroscopic unit, image intensifiers (Hamamatsu Photonics) equipped with a
449 custom-made cooling system, magnification lens system for giving 266.7× final magnification,
450 and EM-CCD cameras (Hamamatsu Photonics) (Kurokawa et al., 2013). Image acquisition was
451 executed by custom-made software (Yokogawa Electric). For 3D images, we collected optical
452 sections spaced 100 nm apart in stacks by oscillating the objective lens vertically with a custom-
453 made piezo actuator. Z stack images were converted to 3D voxel data and processed by
454 deconvolution with Volocity software (Perkin Elmer) using the theoretical point-spread function
455 for spinning-disk confocal microscopy. Imaging analysis was done using Volocity and
456 MetaMorph software (Molecular Devices).

457

458

459

460 **Acknowledgements**

461 We thank members of the Malhotra lab for their valuable discussions. V. Malhotra is an Institució
462 Catalana de Recerca i Estudis Avançats professor at the Centre for Genomic Regulation. This work
463 was funded by grants from the Spanish Ministry of Economy and Competitiveness (BFU2013-
464 44188-P and BFU2016_75372-P to VM) and by Grants-in-Aid for Scientific Research from Japan
465 Society for the Promotion of Science (JP17H06420, and JP18H05275 to AN and KK). We
466 acknowledge support of the Spanish Ministry of Economy, Industry and Competitiveness (MEIC)
467 to the EMBL partnership, the Programmes “Centro de Excelencia Severo Ochoa 2013- 2017”
468 (SEV-2012-0208 & SEV-2013-0347), and the CERCA Programme/Generalitat de Catalunya. This
469 work reflects only the authors’ views, and the EU Community is not liable for any use that may be
470 made of the information contained therein. The authors declare no competing financial interests.

471

472 **Author Contributions**

473 Following the CRediT nomenclature, Amy J. Curwin, Nathalie Brouwers and Kazuo Kurokawa
474 contributed to investigation, and visualization. AJC also contributed to conceptualization, formal
475 analysis, project administration, methodology, validation, writing – original draft and writing –
476 review & editing. Vivek Malhotra and Akihiko Nakano contributed to the conceptualization,
477 funding acquisition, project administration, supervision and writing – original draft and writing –
478 review & editing.

479

480

481

482

483

484

485

486 **References**

- 487
- 488 Bai, L., Kovach, A., You, Q., Hsu, H.-C., Zhao, G., and Li, H. (2019). Autoinhibition and
489 activation mechanisms of the eukaryotic lipid flippase Drs2p-Cdc50p. *Nat. Commun.* *10*, 4142.
490
- 491 Best, J.T., Xu, P., McGuire, J.G., Leahy, S.N., and Graham, T.R. (2020). Yeast synaptobrevin,
492 Snc1, engages distinct routes of postendocytic recycling mediated by a sorting nexin, Rcy1-
493 COPI, and retromer. *Mol. Biol. Cell* *31*, 944–962.
494
- 495 Bruns, C., McCaffery, J.M., Curwin, A.J., Duran, J.M., and Malhotra, V. (2011). Biogenesis of a
496 novel compartment for autophagosome-mediated unconventional protein secretion. *J. Cell Biol.*
497 *195*, 979–992.
498
- 499 Chen, C.-Y., Ingram, M.F., Rosal, P.H., and Graham, T.R. (1999). Role for Drs2p, a P-Type
500 Atpase and Potential Aminophospholipid Translocase, in Yeast Late Golgi Function. *J. Cell Biol.*
501 *147*, 1223–1236.
502
- 503 Chiritoiu, M., Brouwers, N., Turacchio, G., Pirozzi, M., and Malhotra, V. (2019). GRASP55 and
504 UPR Control Interleukin-1 β Aggregation and Secretion. *Dev. Cell* *49*, 145-155.e4.
505
- 506 Cruz-Garcia, D., Curwin, A.J., Popoff, J.-F., Bruns, C., Duran, J.M., and Malhotra, V. (2014).
507 Remodeling of secretory compartments creates CUPS during nutrient starvation. *J. Cell Biol.*
508 *207*, 695–703.
509
- 510 Cruz-Garcia, D., Brouwers, N., Malhotra, V., and Curwin, A.J. (2020). Reactive oxygen species
511 triggers unconventional secretion of antioxidants and Acb1. *J. Cell Biol.* *219*.
512
- 513 Curwin, A.J., Brouwers, N., Adell, M.A.Y., Teis, D., Turacchio, G., Parashuraman, S., Ronchi,
514 P., and Malhotra, V. (2016). ESCRT-III drives the final stages of CUPS maturation for
515 unconventional protein secretion. *ELife* *5*, e16299.
516
- 517 Day, K.J., Casler, J.C., and Glick, B.S. (2018). Budding Yeast Has a Minimal Endomembrane
518 System. *Dev. Cell* *44*, 56-72.e4.
519
- 520 Demmel, L., Beck, M., Klose, C., Schlaitz, A.-L., Gloor, Y., Hsu, P.P., Havlis, J., Shevchenko,
521 A., Krause, E., Kalaidzidis, Y., et al. (2008). Nucleocytoplasmic shuttling of the Golgi
522 phosphatidylinositol 4-kinase Pik1 is regulated by 14-3-3 proteins and coordinates Golgi
523 function with cell growth. *Mol. Biol. Cell* *19*, 1046–1061.
524
- 525 Faulhammer, F., Kanjilal-Kolar, S., Knödler, A., Lo, J., Lee, Y., Konrad, G., and Mayinger, P.
526 (2007). Growth control of Golgi phosphoinositides by reciprocal localization of sac1 lipid
527 phosphatase and pik1 4-kinase. *Traffic Cph. Den.* *8*, 1554–1567.
528
- 529 Furuta, N., Fujimura-Kamada, K., Saito, K., Yamamoto, T., and Tanaka, K. (2006). Endocytic
530 Recycling in Yeast Is Regulated by Putative Phospholipid Translocases and the Ypt31p/32p–
531 Rcy1p Pathway. *Mol. Biol. Cell* *18*, 295–312.

- 532 Gall, W.E., Geething, N.C., Hua, Z., Ingram, M.F., Liu, K., Chen, S.I., and Graham, T.R. (2002).
533 Drs2p-Dependent Formation of Exocytic Clathrin-Coated Vesicles In Vivo. *Curr. Biol.* *12*,
534 1623–1627.
535
- 536 Graham, T.R., and Burd, C.G. (2011). Coordination of Golgi functions by phosphatidylinositol
537 4-kinases. *Trends Cell Biol.* *21*, 113–121.
538
- 539 Hanamatsu, H., Fujimura-Kamada, K., Yamamoto, T., Furuta, N., and Tanaka, K. (2014).
540 Interaction of the phospholipid flippase Drs2p with the F-box protein Rcy1p plays an important
541 role in early endosome to trans-Golgi network vesicle transport in yeast. *J. Biochem. (Tokyo)*
542 *155*, 51–62.
543
- 544 Hankins, H.M., Sere, Y.Y., Diab, N.S., Menon, A.K., and Graham, T.R. (2015).
545 Phosphatidylserine translocation at the yeast trans-Golgi network regulates protein sorting into
546 exocytic vesicles. *Mol. Biol. Cell* *26*, 4674–4685.
547
- 548 He, W., Wan, H., Hu, L., Chen, P., Wang, X., Huang, Z., Yang, Z.-H., Zhong, C.-Q., and Han, J.
549 (2015). Gasdermin D is an executor of pyroptosis and required for interleukin-1 β secretion. *Cell*
550 *Res.* *25*, 1285.
551
- 552 Hua, Z., Fatheddin, P., and Graham, T.R. (2002). An Essential Subfamily of Drs2p-related P-
553 Type ATPases Is Required for Protein Trafficking between Golgi Complex and
554 Endosomal/Vacuolar System. *Mol. Biol. Cell* *13*, 3162–3177.
555
- 556 Kineth, M.A., Anjard, C., Fuller, D., Guizzunti, G., Loomis, W.F., and Malhotra, V. (2007).
557 The Golgi-Associated Protein GRASP Is Required for Unconventional Protein Secretion during
558 Development. *Cell* *130*, 524–534.
559
- 560 Kurokawa, K., Ishii, M., Suda, Y., Ichihara, A., and Nakano, A. (2013). Chapter 14 - Live Cell
561 Visualization of Golgi Membrane Dynamics by Super-resolution Confocal Live Imaging
562 Microscopy. In *Methods in Cell Biology*, F. Perez, and D.J. Stephens, eds. (Academic Press), pp.
563 235–242.
564
- 565 Kurokawa, K., Osakada, H., Kojidani, T., Waga, M., Suda, Y., Asakawa, H., Haraguchi, T., and
566 Nakano, A. (2019). Visualization of secretory cargo transport within the Golgi apparatus. *J. Cell*
567 *Biol.* *218*, 1602–1618.
568
- 569 Lewis, M.J., Nichols, B.J., Prescianotto-Baschong, C., Riezman, H., and Pelham, H.R.B. (2000).
570 Specific Retrieval of the Exocytic SNARE Snc1p from Early Yeast Endosomes. *Mol. Biol. Cell*
571 *11*, 23–38.
572
- 573 Liu, K., Surendhran, K., Nothwehr, S.F., and Graham, T.R. (2008). P4-ATPase Requirement for
574 AP-1/Clathrin Function in Protein Transport from the trans-Golgi Network and Early
575 Endosomes. *Mol. Biol. Cell* *19*, 3526–3535.

- 576 Liu, X., Zhang, Z., Ruan, J., Pan, Y., Magupalli, V.G., Wu, H., and Lieberman, J. (2016).
577 Inflammasome-activated gasdermin D causes pyroptosis by forming membrane pores. *Nature*
578 *535*, 153–158.
- 579
580 Ma, M., and Burd, C.G. (2019). Retrograde trafficking and quality control of yeast
581 synaptobrevin, Snc1, are conferred by its transmembrane domain. *Mol. Biol. Cell* *30*, 1729–
582 1742.
- 583
584 McCullough, J., Clippinger, A.K., Talledge, N., Skowyra, M.L., Saunders, M.G., Naismith, T.V.,
585 Colf, L.A., Afonine, P., Arthur, C., Sundquist, W.I., et al. (2015). Structure and membrane
586 remodeling activity of ESCRT-III helical polymers. *Science* *350*, 1548–1551.
- 587
588 Natarajan, P., Wang, J., Hua, Z., and Graham, T.R. (2004). Drs2p-coupled aminophospholipid
589 translocase activity in yeast Golgi membranes and relationship to in vivo function. *Proc. Natl.*
590 *Acad. Sci.* *101*, 10614–10619.
- 591
592 Natarajan, P., Liu, K., Patil, D.V., Sciorra, V.A., Jackson, C.L., and Graham, T.R. (2009).
593 Regulation of a Golgi flippase by phosphoinositides and an ArfGEF. *Nat. Cell Biol.* *11*, 1421–
594 1426.
- 595
596 Protopopov, V., Govindan, B., Novick, P., and Gerst, J.E. (1993). Homologs of the
597 synaptobrevin/VAMP family of synaptic vesicle proteins function on the late secretory pathway
598 in *S. cerevisiae*. *Cell* *74*, 855–861.
- 599
600 Rowland, A.A., Chitwood, P.J., Phillips, M.J., and Voeltz, G.K. (2014). ER contact sites define
601 the position and timing of endosome fission. *Cell* *159*, 1027–1041.
- 602
603 Schäfer, T., Zentgraf, H., Zehe, C., Brügger, B., Bernhagen, J., and Nickel, W. (2004).
604 Unconventional secretion of fibroblast growth factor 2 is mediated by direct translocation across
605 the plasma membrane of mammalian cells. *J. Biol. Chem.* *279*, 6244–6251.
- 606
607 Shen, D., Yuan, H., Hutagalung, A., Verma, A., Kümmel, D., Wu, X., Reinisch, K., McNew,
608 J.A., and Novick, P. (2013). The synaptobrevin homologue Snc2p recruits the exocyst to
609 secretory vesicles by binding to Sec6p. *J. Cell Biol.* *202*, 509–526.
- 610
611 Timcenko, M., Lyons, J.A., Janulienė, D., Ulstrup, J.J., Dieudonné, T., Montigny, C., Ash, M.-
612 R., Karlsen, J.L., Boesen, T., Kühlbrandt, W., et al. (2019). Structure and autoregulation of a P4-
613 ATPase lipid flippase. *Nature* *571*, 366–370.
- 614
615 Tojima, T., Suda, Y., Ishii, M., Kurokawa, K., and Nakano, A. (2019). Spatiotemporal dissection
616 of the trans-Golgi network in budding yeast. *J. Cell Sci.* *132*.
- 617
618 Tsai, P.-C., Hsu, J.-W., Liu, Y.-W., Chen, K.-Y., and Lee, F.-J.S. (2013). Arl1p regulates spatial
619 membrane organization at the trans-Golgi network through interaction with Arf-GEF Gea2p and
620 flippase Drs2p. *Proc. Natl. Acad. Sci. U. S. A.* *110*, E668–677.

621 Villeneuve, J., Bassaganyas, L., Lepreux, S., Chiritoiu, M., Costet, P., Ripoche, J., Malhotra, V.,
622 and Schekman, R. (2017). Unconventional secretion of FABP4 by endosomes and secretory
623 lysosomes. *J Cell Biol* jcb.201705047.
624
625 Walch-Solimena, C., and Novick, P. (1999). The yeast phosphatidylinositol-4-OH kinase Pik1
626 regulates secretion at the Golgi. *Nat. Cell Biol.* *1*, 523–525.
627
628 Zhang, M., Liu, L., Lin, X., Wang, Y., Li, Y., Guo, Q., Li, S., Sun, Y., Tao, X., Zhang, D., et al.
629 (2020). A Translocation Pathway for Vesicle-Mediated Unconventional Protein Secretion. *Cell*
630 *181*, 637-652.e15.
631
632 Zhou, X., Sebastian, T.T., and Graham, T.R. (2013). Auto-inhibition of Drs2p, a yeast
633 phospholipid flippase, by its carboxyl-terminal tail. *J. Biol. Chem.* *288*, 31807–31815.
634
635

636 **Figure 1. Drs2 is required for CUPS biogenesis**

637 (A) Cells genomically expressing Drs2-3xGFP and Grh1-2xCherry were visualized by confocal
638 spinning disk microscopy in growth conditions and starvation by incubation in 2% potassium
639 acetate. Short movies were acquired at 10 second intervals to assess the frequency and duration
640 of co-localization. Scale bar = 2 μ m.

641 (B) Wild type and *drs2 Δ* cells expressing Grh1-2xGFP were visualized by epifluorescence
642 microscopy in growth conditions and after incubation in 2% potassium acetate for the indicated
643 times. Cells were classified with normal CUPS (1-3 larger foci per cell); intermediate CUPS
644 (“int.”), where a large focus is observed in addition to smaller structures; and vesiculated CUPS
645 (“ves.”) where only small foci of Grh1 are observed. Scale bar = 2 μ m.

646

647 **Figure 2. Drs2-Rcy1 pathway and the v-SNAREs, Snc1 and Snc2, are required for CUPS**
648 **formation**

649 Wild type and the indicated deletion or mutant strains expressing Grh1-2xGFP were visualized
650 by epifluorescence microscopy in growth conditions and after incubation in 2% potassium
651 acetate for the indicated times. Cells were classified with normal CUPS (1-3 larger foci per cell),
652 intermediate CUPS (“int.”); where a large focus is observed in addition to smaller structures, and
653 vesiculated CUPS (“ves.”); where only small foci of Grh1 are observed. Scale bar = 2 μ m.

654

655 **Figure 3. Rcy1 and v-SNAREs are required for unconventional secretion**

656 (A+B) Wild type, *rcy1* Δ or *snc1* Δ *snc2-V39A*, *M42A* cells were grown logarithmic phase,
657 washed twice and cultured in 2% potassium acetate for 2.5 hours. The cell wall proteins were
658 extracted from equal number of cells followed by precipitation with TCA (“secreted”). Lysates
659 and secreted proteins were analyzed by western blot and the ratio of the secreted/lysate for the
660 indicated protein was determined and compared to that of wild type in each experiment.
661 Statistical analyses were performed for the indicated unconventional cargo proteins and the
662 reduction in secretion compared to wild type is indicated \pm standard deviation.

663

664 **Figure 4. CUPS contain a pool of the v-SNARE Snc2 and the t-SNARE Tlg2**

665 (A) Cells genomically expressing Grh1-2xCherry with GFP-Snc1, GFP-Snc2 or GFP-Tlg2 were
666 visualized by confocal spinning disk microscopy in growth conditions and (B) throughout the
667 time course of culture in 2% potassium acetate. Short movies were acquired at 10 second
668 intervals to assess the frequency and duration of co-localization. Scale bar = 2 μ m.

669

670 **Figure 5. SCLIM reveals the dynamic structure of CUPS**

671 (A) Grh1-2xGFP cells were incubated in normal growth conditions or 2% potassium acetate for
672 3 hours and visualized by SCLIM. In growth, Grh1 labelled many small and mobile structures
673 (early Golgi membranes and ER-exit sites). In starvation, Grh1 labelled fewer, larger, and less
674 mobile membrane structures (CUPS) Grid = 1.52 μ m

675 (B) Line scan analysis in 3D of multiple CUPS structures revealed three forms; spherical (3/14),
676 complex curved (8/14) or cup-shaped (3/14).

677 (C) Visualization of CUPS over time showed stable, mature CUPS are still dynamic, able to
678 change morphology between the different forms. Arrows = non-moving structures; dotted circles
679 = moving structures. Red circle is the region in the time-lapse images at 25, 50 and 75 frames.
680 Movies 1-4; regions 1-3 and red circle region. 20 sec intervals, 60x speed.

681

682 **Figure 6. SCLIM analysis of Drs2 and Tlg2 labelled structures in growth (TGN) and**
683 **starvation (TCUPS)**

684 (A) Drs2-3xCherry (magenta) and GFP-Tlg2 (green) cells were visualized in growth condition.
685 White indicates co-localization. Time-lapse images of the two regions indicated. Movie 5, 4 sec
686 intervals, 20x speed.

687 (B) Drs2-3xCherry (magenta) and GFP-Tlg2 (green) cells were visualized at 2 hours starvation.
688 White indicates co-localization. Time-lapse images of the two cells indicated. Movie 7- zoomed
689 out and Movies 8-9 – zoomed in of two indicated regions, 10 sec intervals, 20x speed.

690

691 **Figure 7. SCLIM analysis of CUPS-TCUPS contacts**

692 (A) Grh1-2xCherry (magenta) and GFP-Tlg2 (green) cells cultured in starvation condition 1.5
693 hours. 3D time-lapse images (20 sec intervals). White arrowheads show separated membrane
694 structures labeled with GFP-Tlg2. Yellow arrowheads indicate where the membrane structures
695 have been cut. White arrows indicate where Grh1 contacts with Tlg2 protrusive membrane. Scale
696 bar=0.5 μ m. Movie 9, 20 sec intervals, 20x speed.

697 (B) Grh1-2xCherry (magenta) and Drs2-3xGFP (green) cells cultured in starvation condition 1.5
698 hours. 3D time-lapse images (10 sec intervals). White arrowheads show separated membrane
699 structures labeled with Drs2-3xGFP. Yellow arrowheads indicate where the membrane structures

700 have been cut. White arrows indicate where Grh1 contacts with Drs2 protrusive membrane.

701 Scale bar=0.5 μ m. Movie 10, 10 sec intervals, 20x speed.

702

703 **Figure 8. A working scheme building CUPS-TCUPS for unconventional secretion**

704 During growth, cells predominantly depend on the conventional ER-Golgi pathway of protein

705 secretion. When cells are cultured in starvation medium, there is a sharp reduction in the use of

706 conventional secretory pathway and the cells switch to a new or an unconventional mode to

707 release essential proteins to cell's exterior. A cis Golgi membrane produces small fragments, that

708 do not contain glycosylation enzymes, in a COPI independent manner to synthesize CUPS

709 (magenta). The early TGN produces small membranes to generate a compartment that we have

710 called TCUPS (green). Our data show that tubules emanating from TCUPS are collared by

711 CUPS, which is followed by severing of the tubule. We suggest that these contacts, over a

712 period, lead to the consumption of TCUPS to produce smaller elements (vesicles + tubules).

713 These smaller elements are likely used for delivering essential proteins to other compartments of

714 the cell and release proteins like SOD1 and Acb1 to cell's exterior. This mode of TGN

715 consumption is common to both the conventional and unconventional protein secretion

716 processes. Upon shifting cells to growing conditions, components of the CUPS are delivered by

717 COPI vesicles to the ER, which then traffic the respective components to the Golgi, thereby

718 restoring the Golgi to restart the conventional mode of protein secretion.

719

720 **Figure S1. No CUPS defect in cells lacking Gea2, Arl1, Chc1, Apl6, Aps1, Snc1 or Snc2**

721 The indicated deletion strains expressing Grh1-2xGFP were grown to log phase and starved for

722 2.5h. Scale bar = 2 μ m

723 **Figure S2. Drs2, Tlg2 and Snc2 label the same compartment in starvation – TCUPS**

724 Cells co-expressing GFP-Tlg2 with Drs2-3xmCherry or mCherry-Snc2 were visualized by
725 spinning disk confocal microscopy in the indicated conditions. In both combinations the average
726 Pearson's coefficient increased from ~0.3 in growth to ~0.7 in starvation (n=25-40 cells). Scale
727 bar = 2 μ m.

728

729 **Figure S3. Drs2 and Snc2 also label small vesicles that contact with, or are near CUPS**

730 Grh1-2xCh (magenta) cells co-expressing either (A) Drs2-3xGFP (green) or (B) GFP-Snc2
731 (green) were cultured in starvation condition for 1 hour. Movies S4-8; 10 sec intervals, 20x
732 speed.

733

734 **Supplemental movies 1-3. CUPS form by dynamic fusion and fission of existing membranes.**

735 Grh1-2xCherry (magenta) with GFP-Snc2 (green) at 1 hour of starvation. Movie S1 - smaller
736 Grh1 structures can fuse. Movies S2 and S3 – larger Grh1 structures can separate and disperse.
737 10 sec intervals, 20x speed.

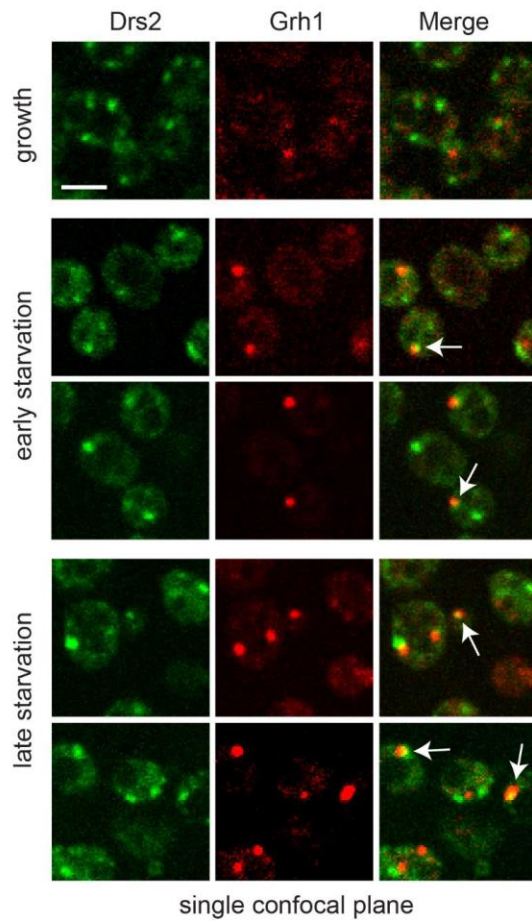
738

739

740

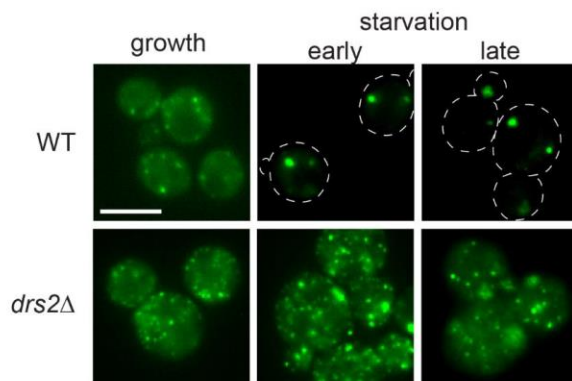
Figure 1

A



time	CUPS with co-loc	n
early (0 - 1h)	26%	299
late (1 - 2.5h)	10%	256

B



early (30 - 45 min)

strain	CUPS	int.	ves.	n
WT	87%	10%	3%	67
<i>drs2Δ</i>	0%	18%	82%	55

late (2.5 - 3h)

strain	CUPS	int.	ves.	n
WT	89%	7%	4%	44
<i>drs2Δ</i>	0%	17%	83%	57

Figure 2

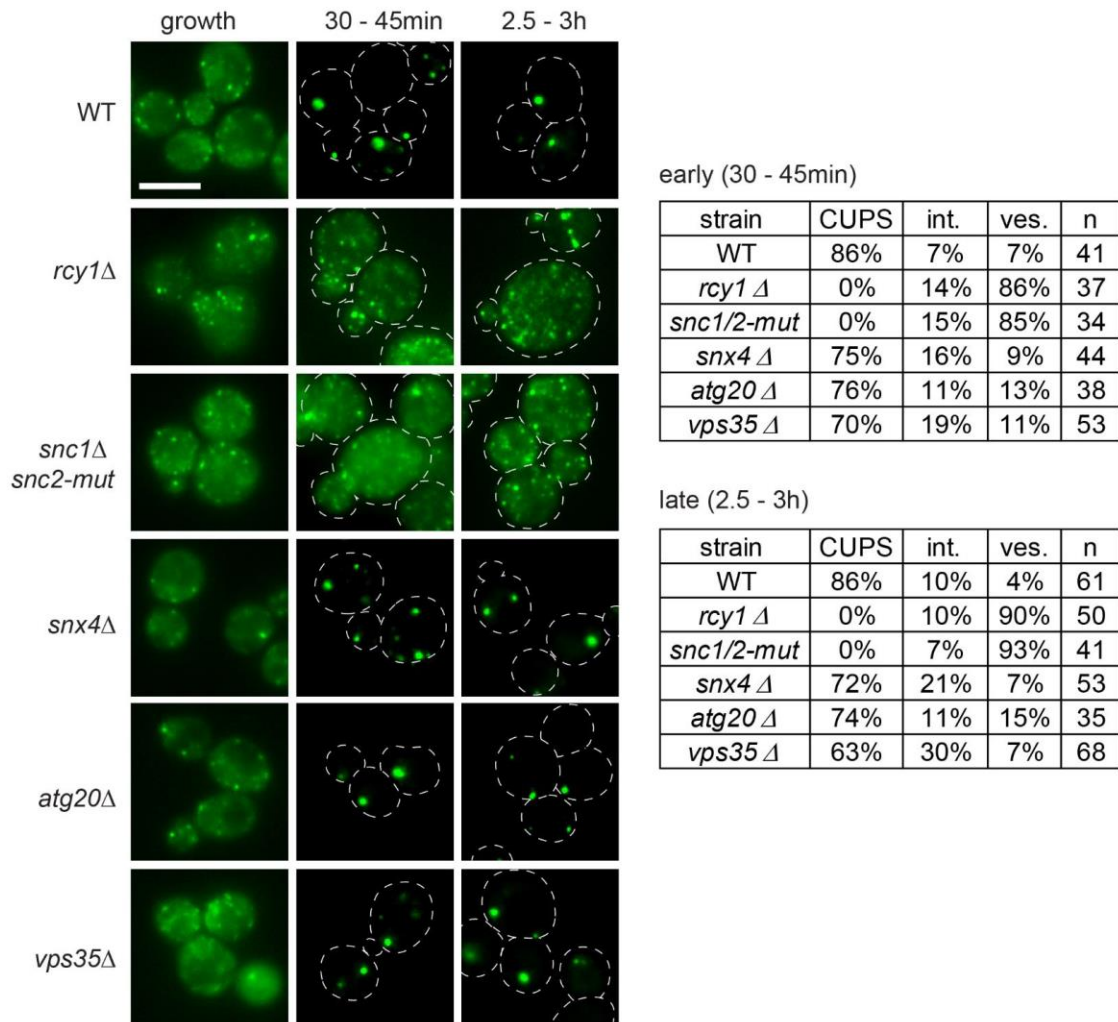
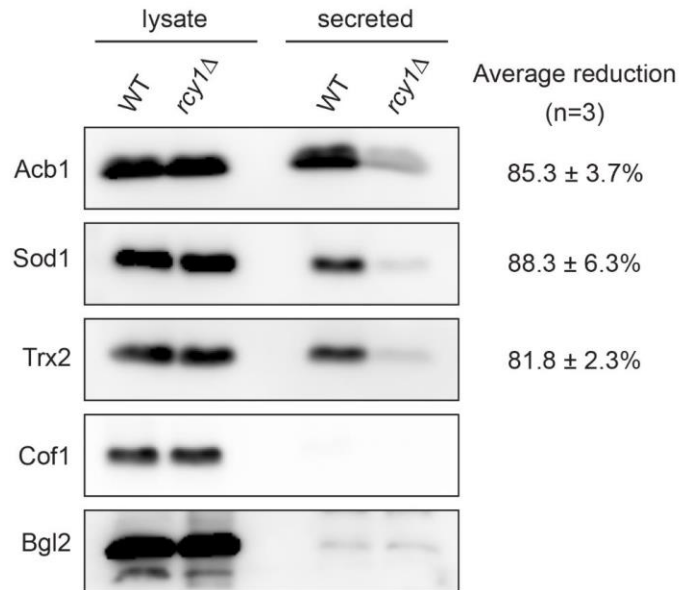
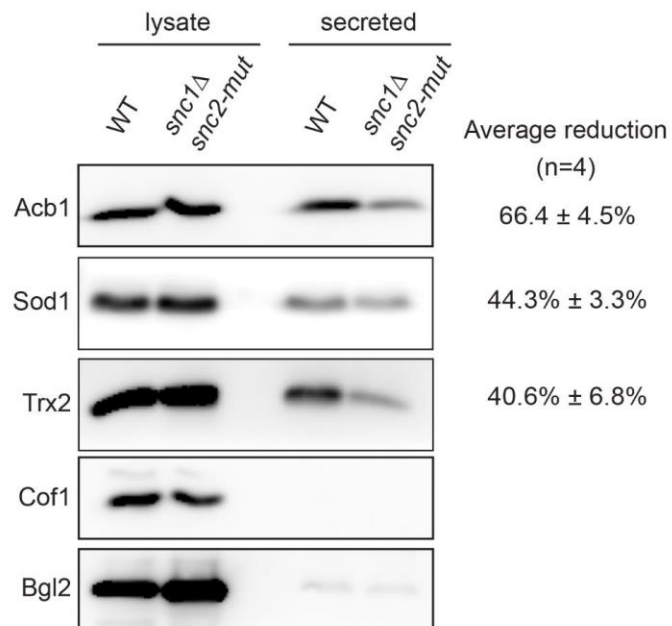


Figure 3

A



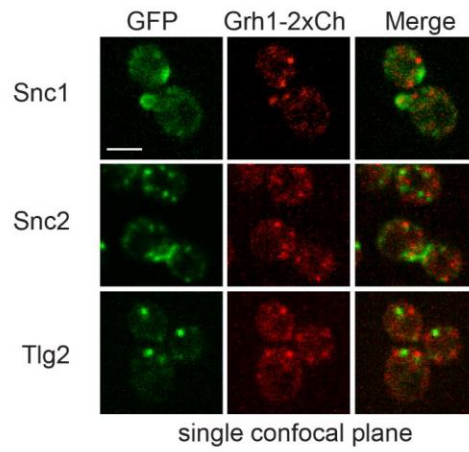
B



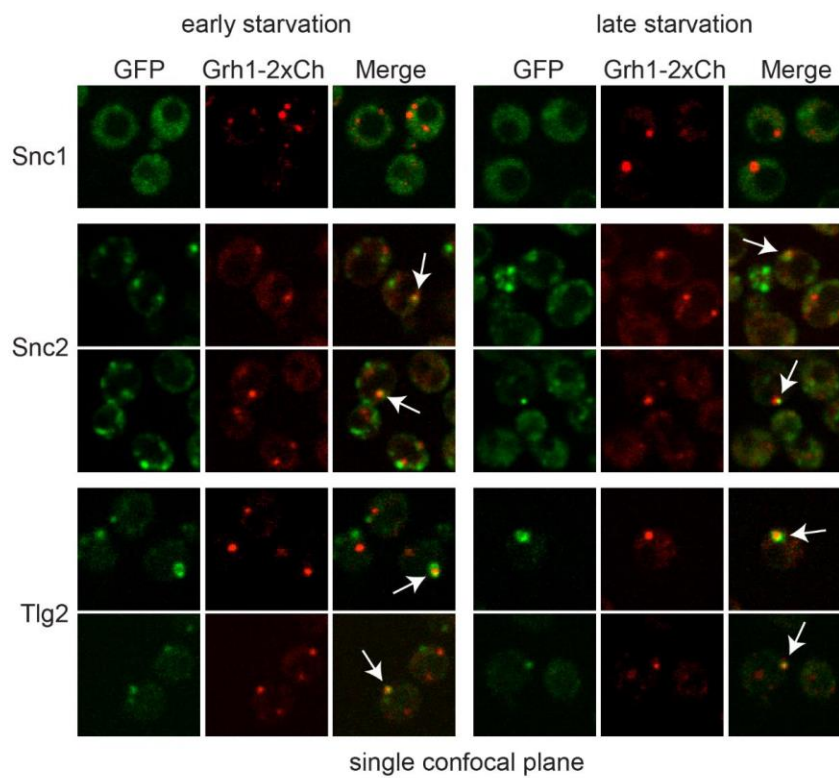
744

Figure 4

A



B



Snc2		
time	CUPS with co-loc	n
early (0 - 1h)	14%	125
late (1 - 2.5h)	12%	139

Tlg2		
time	CUPS with co-loc	n
early (0 - 1h)	14%	110
late (1 - 2.5h)	7%	136

Figure 5

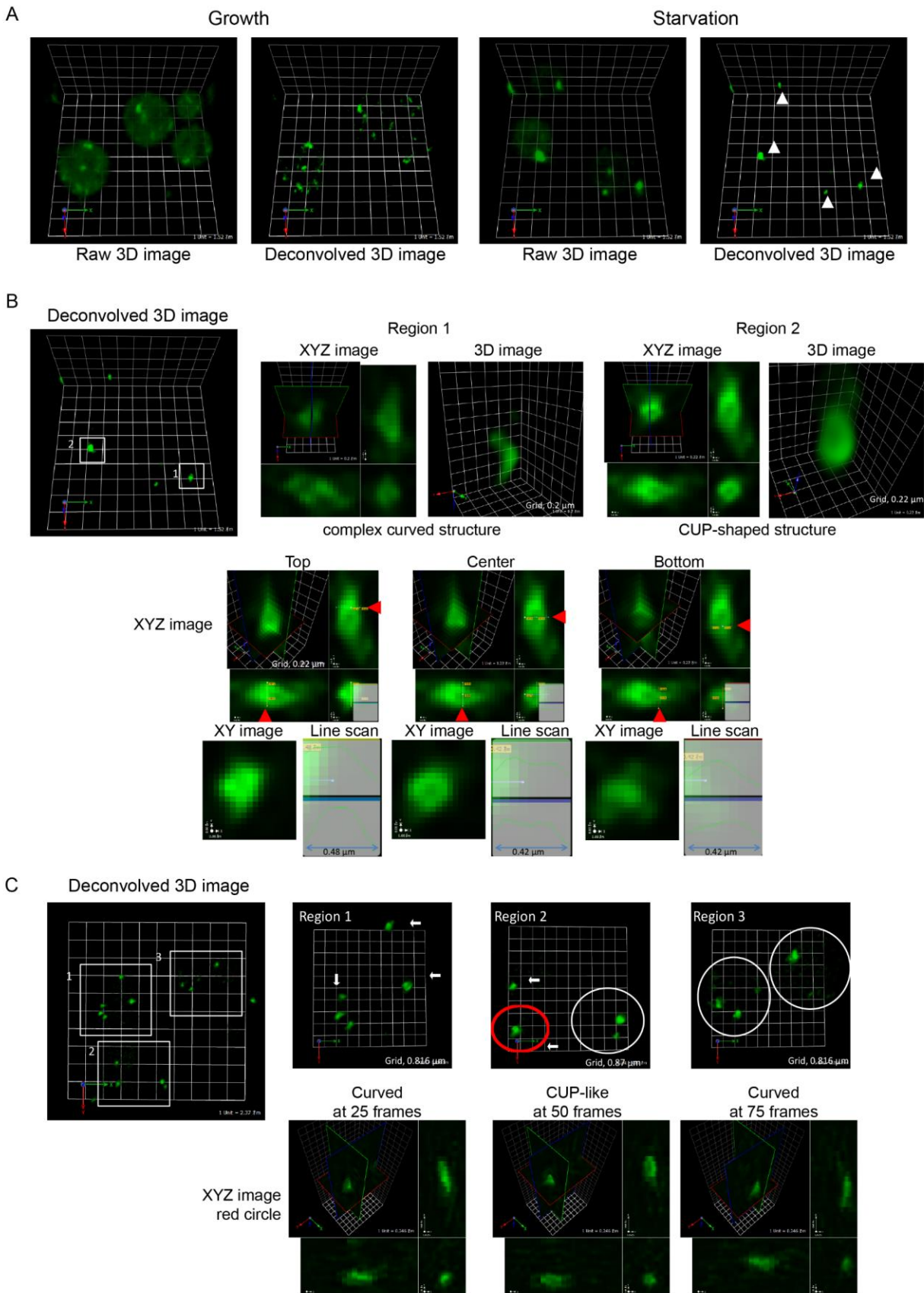
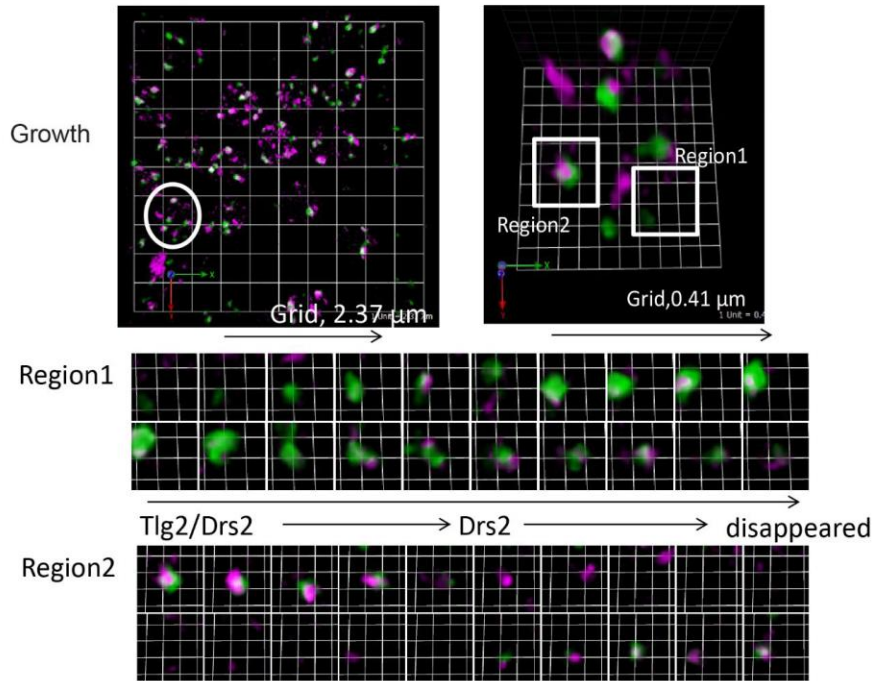
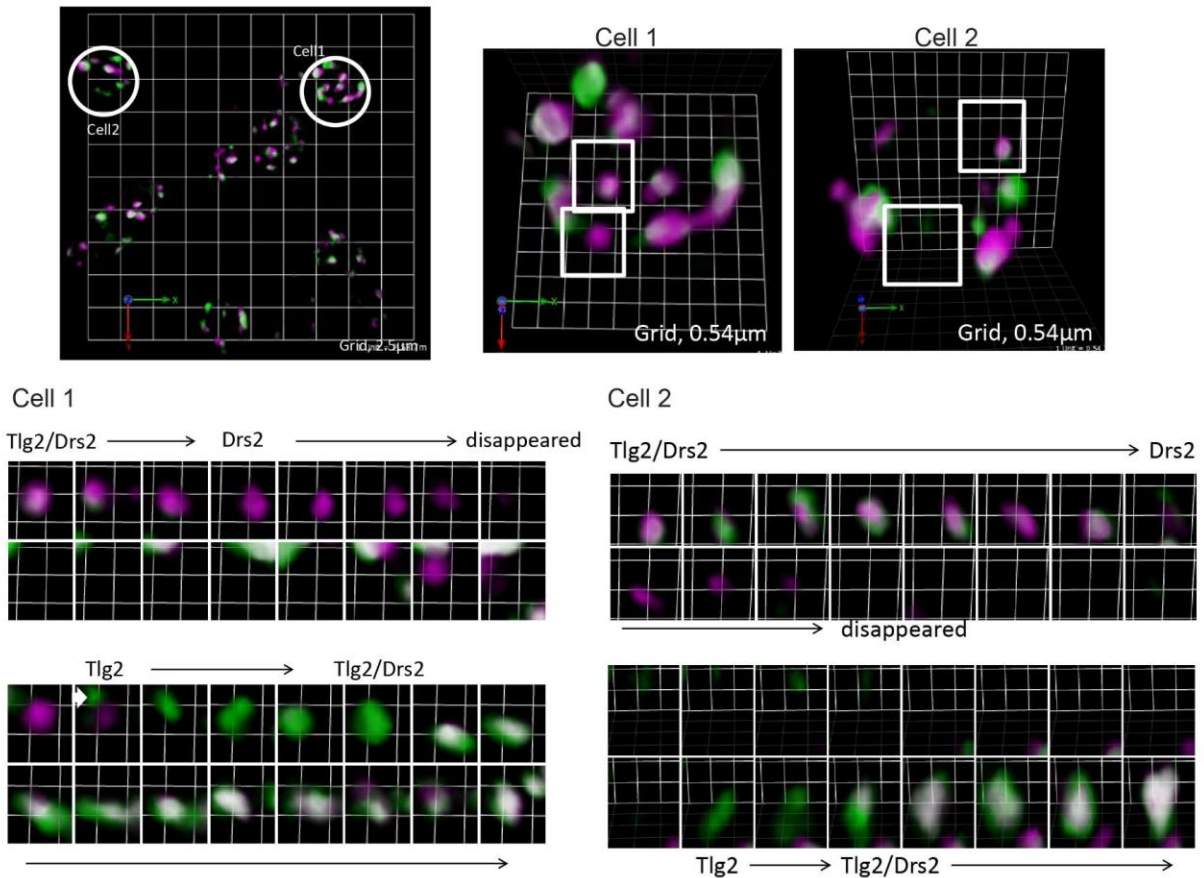


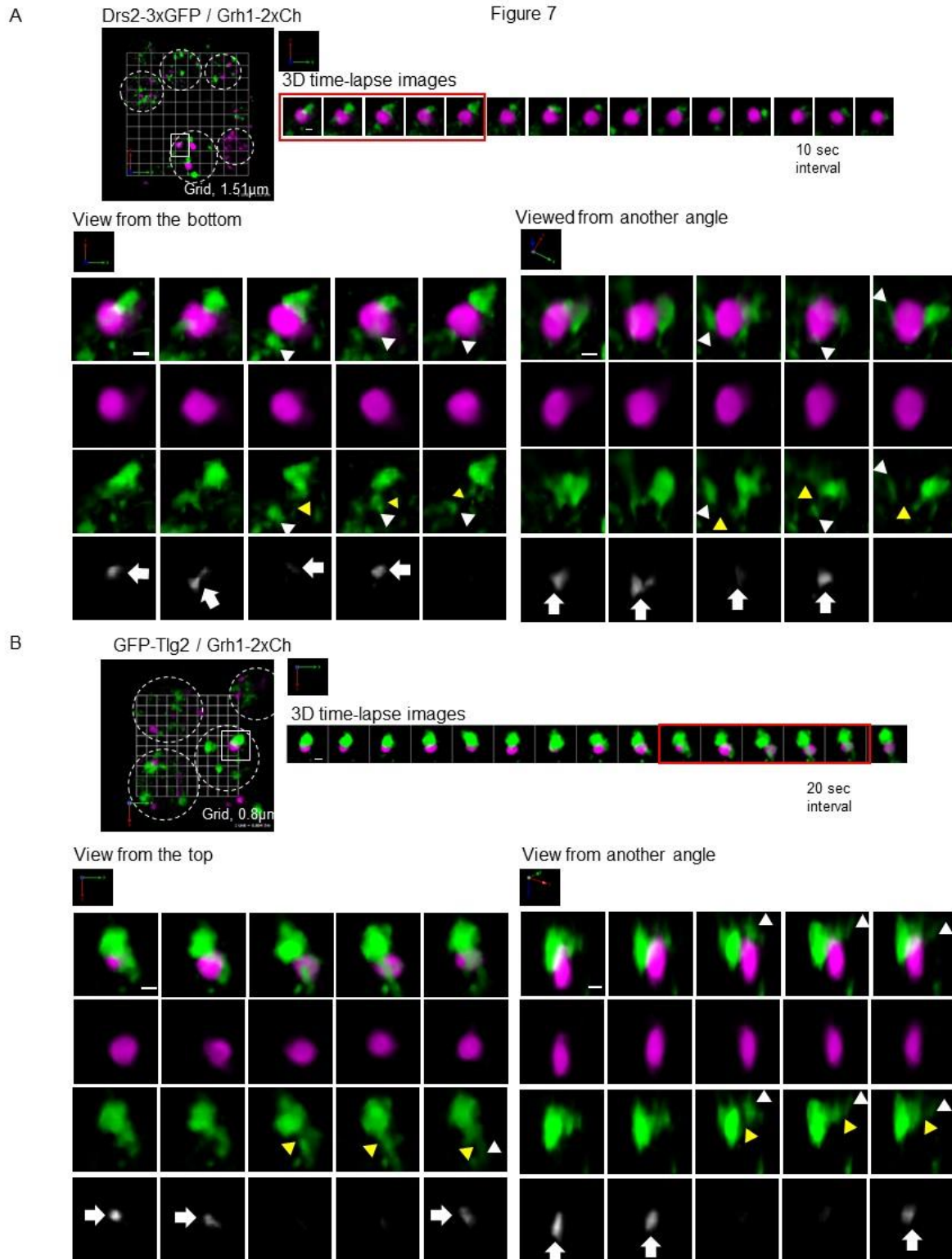
Figure 6

A Drs2-3xmCherry (magenta) and GFP-Tlg2 (green)



B Drs2-3xmCherry and GFP-Tlg2 starvation





748

Figure 8

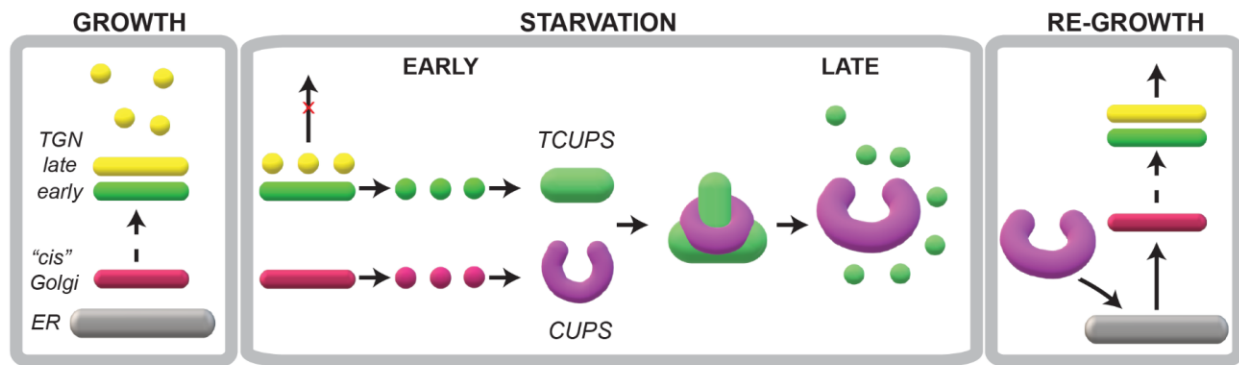


Figure S1

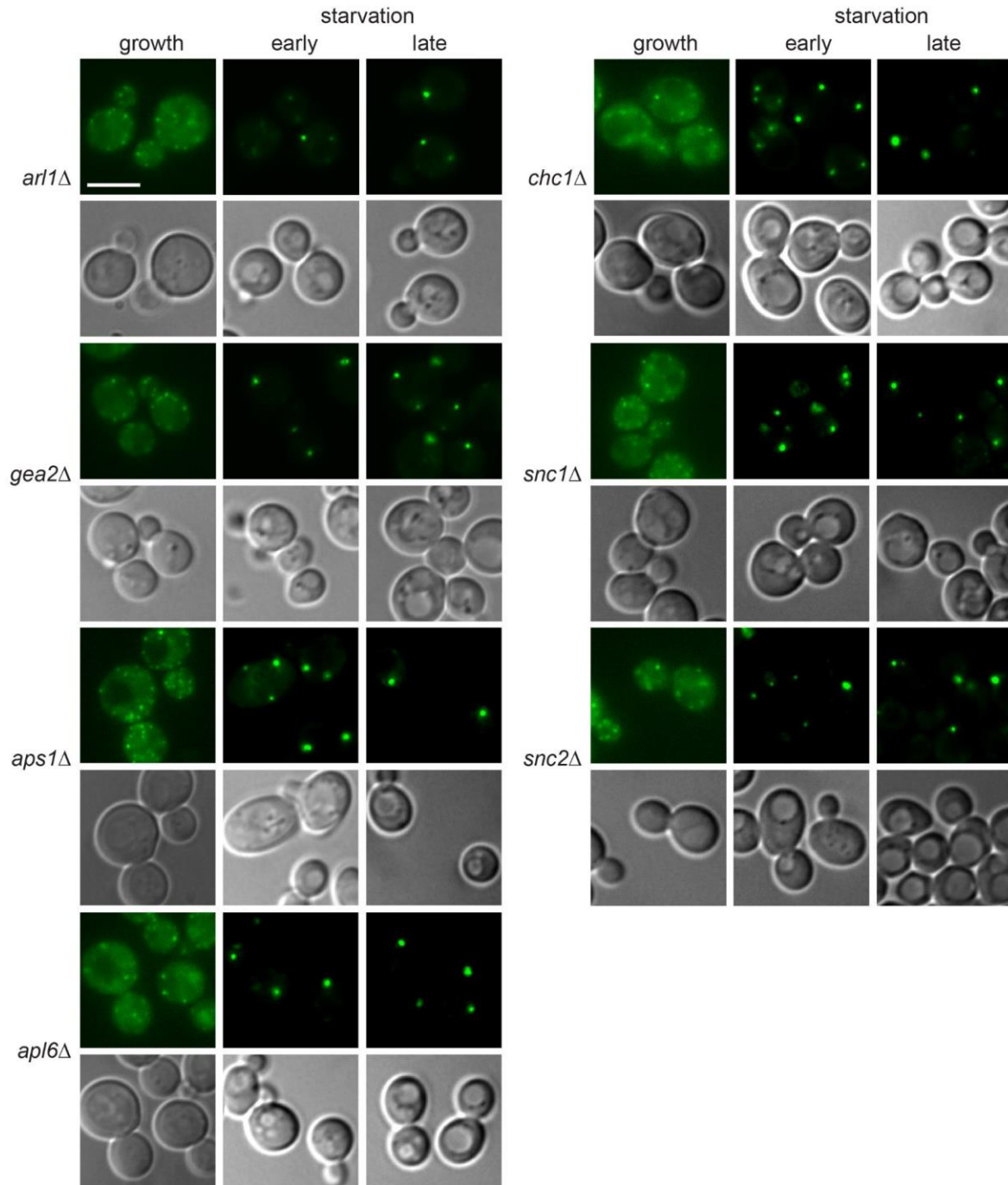


Figure S2

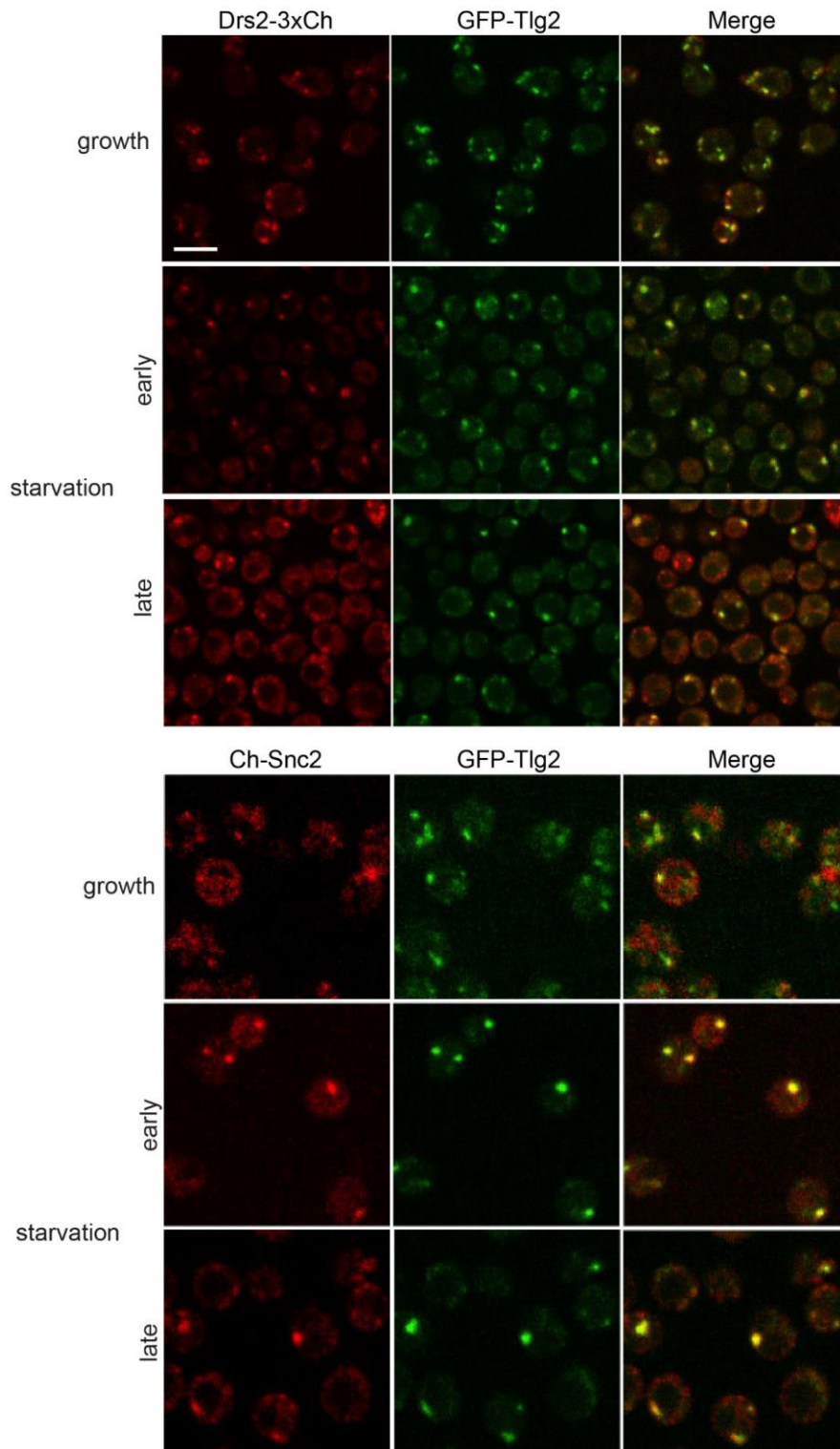
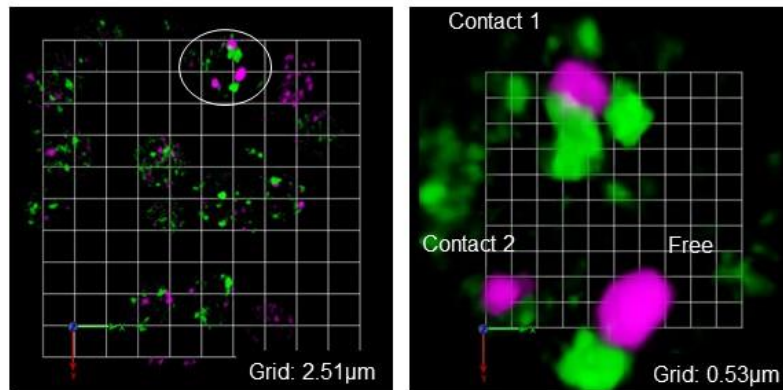


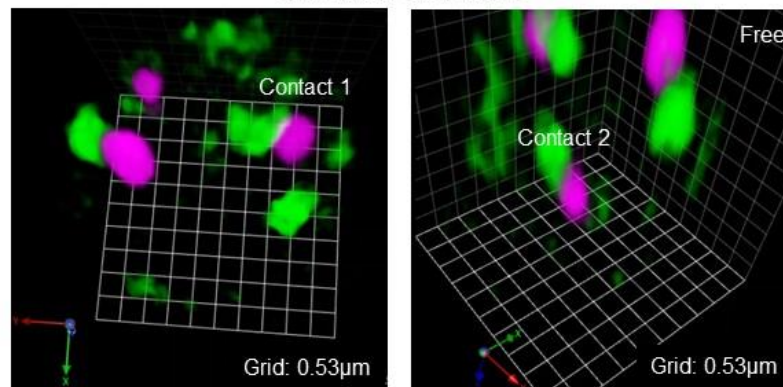
Figure S3

A

Drs2-3xGFP / Grh1-2xCh

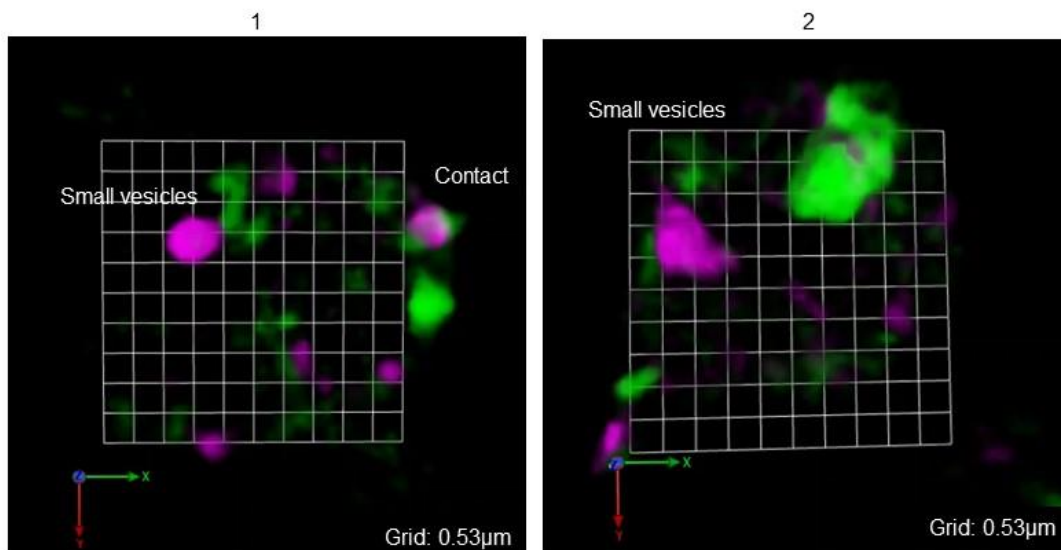


Viewed from other angles



B

GFP-Snc1 / Grh1-2xCh



752